

**LASER INTERFEROMETER GRAVITATIONAL WAVE OBSERVATORY
--LIGO--**

California Institute of Technology
Massachusetts Institute of Technology

Document Number: **LIGO- T030231-00-R** Date: 9/30/2003

Author: Naman Bhatt

**Characterization, Commissioning and
Implementation of the Optical Lever System
at Caltech's 40m Advanced LIGO Prototype
Lab**

**This is an internal working note
of the LIGO Laboratory.**

California Institute of Technology
LIGO Laboratory, MS 18-34
1200 E. California Blvd.
Pasadena, CA 91125
Phone (626) 395-3064
Fax (626) 304-9834

Massachusetts Institute of Technology
LIGO Laboratory, NW17-161
175 Albany St.
Cambridge, MA 01239
Phone (617) 253-4824
Fax (617) 253-7014

LIGO Hanford Observatory
P.O. Box 159
Richland, WA 99352
Phone (509) 372-8106
Fax (509) 372-8137

LIGO Livingston Observatory
P.O. Box 940
Livingston, LA 70754
Phone (225) 686-3100
Fax (225) 686-7189

Characterization, Commissioning and Implementation of the Optical Lever System at Caltech's 40m Advanced LIGO Prototype Laboratory

Author: Naman Bhatt, Caltech

Mentor: Alan Jay Weinstein

LIGO SURF 2003

Abstract

The optical lever (oplev) system is one of the auxiliary optics support systems at the 40m Advanced LIGO prototype at Caltech. There is an oplev for each of the seven suspended optics in the interferometer. Each system is composed of a laser transmitter, optical steering mirrors inside and outside of vacuum, an optical receiver in the form of a segmented photodetector, and a telescope to isolate angle sensing. This report details the characterization and commissioning of detectors and electronics for the oplevs. The characterization includes modeling the system from sensed changes in angular pitch and yaw of the suspended optics through the telescope to feedback on the optics to damp their motion. Commissioning of the oplevs involves assembling and calibrating each optical lever, closing the loop, and demonstrating improved pitch and yaw damping of the suspended optics.

Table of Contents

1	Introduction.....	4
2	Background on the Optical Lever System.....	4
3	Theory Behind the Optical Lever System.....	6
	3.1 Response.....	6
	3.2 Angle-sensing Telescope.....	11
4	Assembly of the Optical Lever System.....	12
	4.1 Mirrors.....	12
	4.2 Beam Path.....	14
	4.3 Electronics.....	15
5	Results and Further Work.....	15
	5.1 Results.....	15
	5.2 Further Work.....	16
	Acknowledgements.....	17
	References.....	18
	Appendix A.....	19
	Appendix B.....	23
	Appendix C.....	32
	Appendix D.....	33

1. Introduction

The Laser Interferometer Gravitational-Wave Observatory (LIGO) is dedicated to detecting gravitational waves and using them to map the universe in an entirely new way. There are two LIGO facilities currently up and running in Livingston, Louisiana and Hanford, Washington that work in conjunction with each other to make detections and locate their sources on the sky. Each detector is in the form of a Michelson interferometer with 4km Fabry-Perot arms. The Hanford site actually has two Michelson interferometers, one with 4km arms and the other with 2km arms. At Caltech, a prototype for Advanced LIGO with 40m arms is being developed. This Michelson detector is an L-shaped device that is designed to detect gravitational waves using optical resonant cavities. Gravitational waves compress space-time in one dimension while expanding it in another. When a wave passes through the interferometer, it changes the lengths of the arms, disturbing the resonance in the cavities. A detection is made in this manner.

My project for the summer was to help design and setup one of the subsystems of the prototype detector, referred to as the optical lever system (oplevs). The ultimate goal is to use the oplevs to help damp the angular motion (pitch and yaw) of the suspended optics in the LIGO interferometer and monitor and maintain the angular orientation of the optics relative to an external reference frame. This makes them an important tool for keeping the interferometer in perfect resonance, commonly referred to as "in lock". When resonance is maintained, the optical cavities of the interferometer will be able to function as sensitive detectors of the space-time distortions caused by gravitational waves.

This report will give an overview of the mathematical background of the optical lever system, describing how they work, and it will detail the various steps in the process of getting this subsystem implemented.

2. Background on the Optical Lever System

Within LIGO's interferometer, there are several optical suspensions that serve to direct the input laser beam and create, maintain, and build up resonance. These optics are placed on suspensions to minimize their motion as much as possible. It is very important that the optics remain as motionless as possible so that they can create perfectly resonant optical cavities. In the diagram of Advanced LIGO below (Figure 2.1), the seven suspended masses are shown: beam splitter (BS), PRM (power-recycling mirror), SRM (signal-recycling mirror), ITM_x and ITM_y (initial test masses for x and y arms), and ETM_x and ETM_y (end test masses for x and y arms).

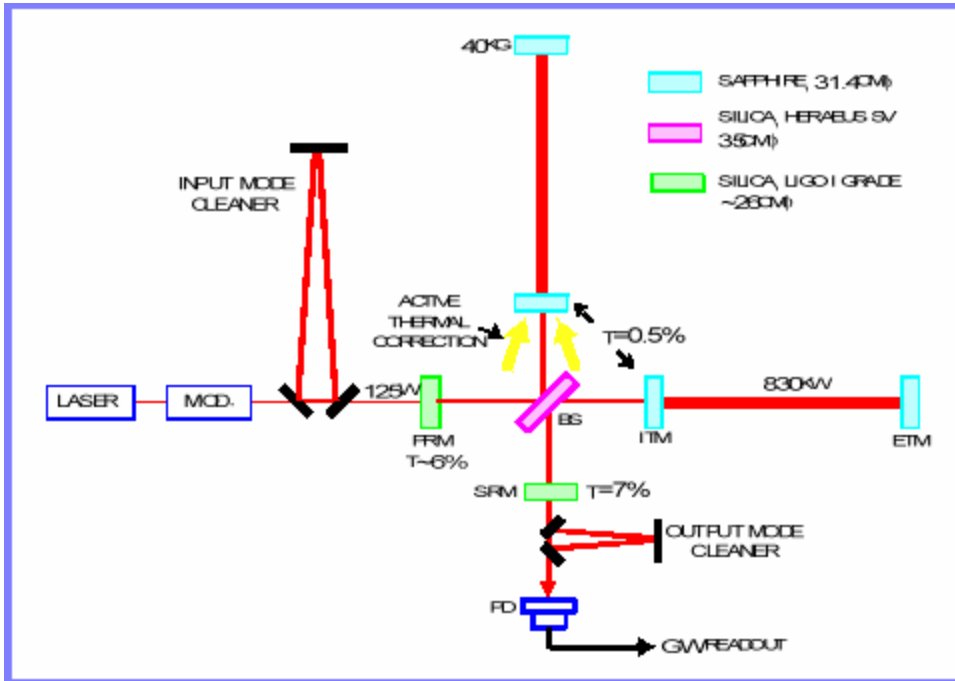


Figure 2.1: Advanced LIGO

In the optical lever system, low-powered laser beams from outside the high vacuum chambers of the interferometer are sent inside through a window and directed at each of the seven inner suspended optics. These beams then reflect off and leave the interferometer through the same window. They are directed to quad photodiodes (QPDs) from which a signal is received. A separate signal is received for each quadrant of the photodiode. By analyzing this signal, we are able to detect angular movement of the suspended optics. The optical lever system uses these signals as input sensors of feedback servos for the optics to make the appropriate compensation based on the angular position measured in two directions, pitch and yaw. The oplevs are designed to help keep the optics in a relatively motionless state with stable angular orientation.

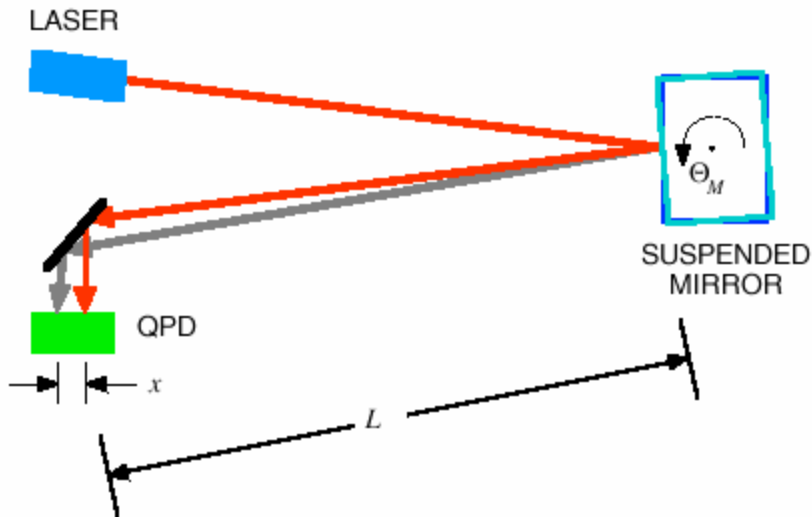


Figure 2.2: Optical lever angle readout for a suspended mirror

In Figure 2.2 above, the QPD is sensitive not only to angular changes but also to positional changes in the motion of the mirror. In order to make the optical lever insensitive to positional change, the final arrangement places a long-focal-length telescope in the beam path directly before the QPD. The telescope consists of a series of lenses. The QPD is placed at the focal length of the last lens (one focal length's distance from the lens). This placement and the inclusion of the telescope in the oplev effectively lengthens the lever arm, which makes it more sensitive to small changes in the mirror's angular orientation, and makes the setup sensitive only to *angular* changes in pitch in yaw.

3. Theory behind the Optical Lever System

3.1. Response

The face of each of the QPDs in each of the seven oplevs looks like a circle split into four quadrants, as in Figure 3.1.1.

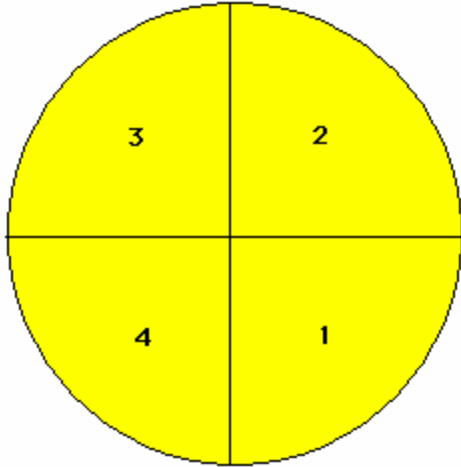


Figure 3.1.1: Circular quadrant photodiode; diameter = 10mm

The four segments of the QPD give four separate photocurrent signals proportional to the amount of light falling in each particular quadrant. The photocurrent in each quadrant is proportional to the amount of optical laser power falling on the photodiode. Each quadrant has a responsivity, R , and transimpedance amplifier, Z , which turns the photocurrents into readout voltages. Using the readout voltages from each quadrant, we are then able to obtain pitch and yaw readings in the following manner:

$$\text{Pitch} = ((2+3)-(1+4)) / (1+2+3+4) \quad (\text{top - bottom}) \quad \text{Equation 1}$$

$$\text{Yaw} = ((1+2)-(3+4)) / (1+2+3+4) \quad (\text{right - left}) \quad \text{Equation 2}$$

In the following printout of the readout signals received from the BS QPD (Figure 3.1.2), pitch is arbitrarily defined as (bottom-top). Yaw continues to be defined as (right-left).

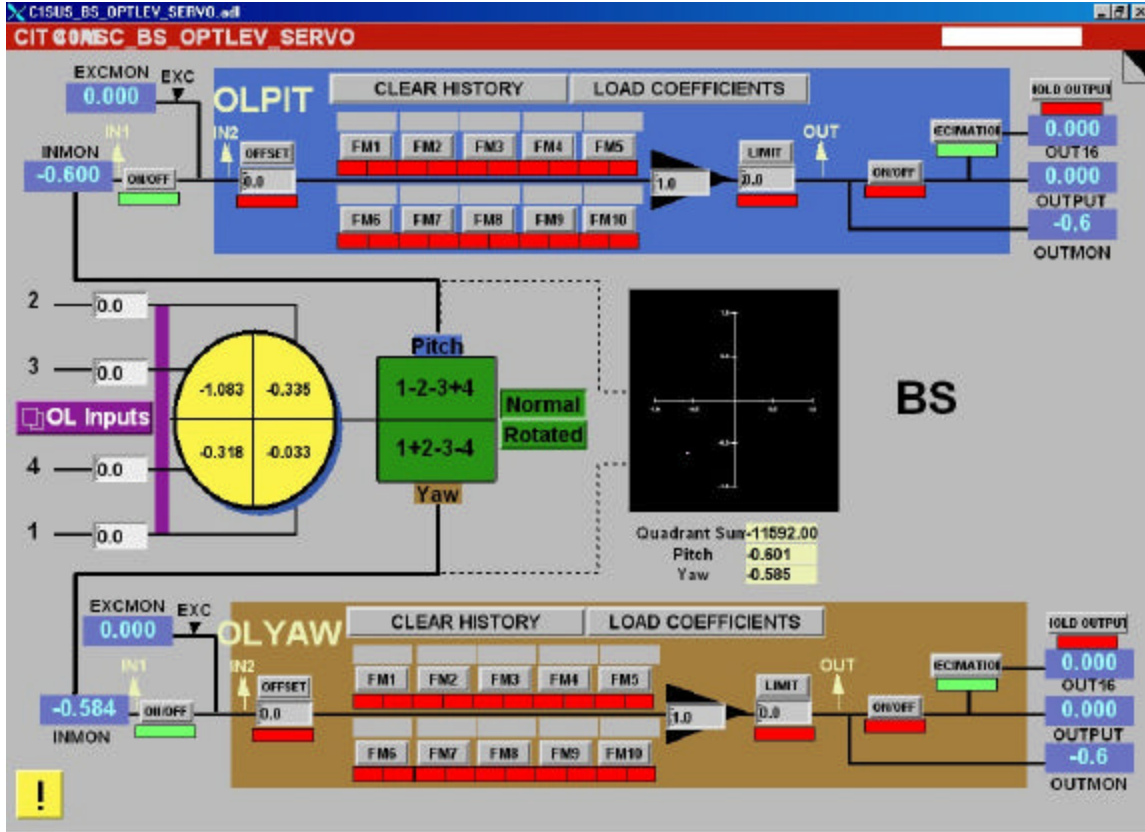


Figure 3.1.2: EPICS display of BS oplev readings

The circular QPD figure in Figure 3.1.2 shows the readout voltages of each quadrant. The Cartesian plane to the right shows pitch and yaw as defined on the screen. The quadrant sum in counts is also given, as well as pitch and yaw as defined by equations 1 and 2.

The laser beam hitting the QPD has a Gaussian intensity profile. We assume that the beam has an ideal Gaussian profile corresponding to the TEM₀₀ mode. The power in each of the four quadrants of the QPD is defined by the following double integrals of intensity:

$$P1(h, k, w, r) = \int_{-r}^0 \int_0^{\sqrt{(r^2 - y^2)}} \text{Exp}\left[\left(\frac{-2}{w^2}\right) * ((x - h)^2 + (y - k)^2)\right] dx dy$$

Equation 3

$$P2(h, k, w, r) = \int_0^r \int_0^{\sqrt{(r^2 - y^2)}} \text{Exp}\left[\left(\frac{-2}{w^2}\right) * ((x - h)^2 + (y - k)^2)\right] dx dy$$

Equation 4

$$P3(h, k, w, r) = \int_0^r \int_{-\sqrt{(r^2 - y^2)}}^0 \text{Exp}\left[\left(\frac{-2}{w^2}\right) * ((x - h)^2 + (y - k)^2)\right] dx dy$$

Equation 5

$$P4(h, k, w, r) = \int_{-r}^0 \int_{-\sqrt{(r^2 - y^2)}}^0 \text{Exp}\left[\left(\frac{-2}{w^2}\right) * ((x - h)^2 + (y - k)^2)\right] dx dy$$

Equation 6

In the above equations, ‘h’ and ‘k’ are coordinates in the x,y-plane, respectively. ‘h’ denotes changes in yaw; ‘k’ in pitch. ‘w’ is the beam waist, defined as the radius at which the Gaussian beam amplitude drops to 1/e of its maximum value. ‘r’ is the radius of the QPD. The total power falling on the QPD is simply the sum of the power falling in each quadrant:

$$\text{Sum}(h, k, w, r) = P1 + P2 + P3 + P4 \quad \text{Equation 7}$$

Below is a 3D representation of the power falling on the QPD.

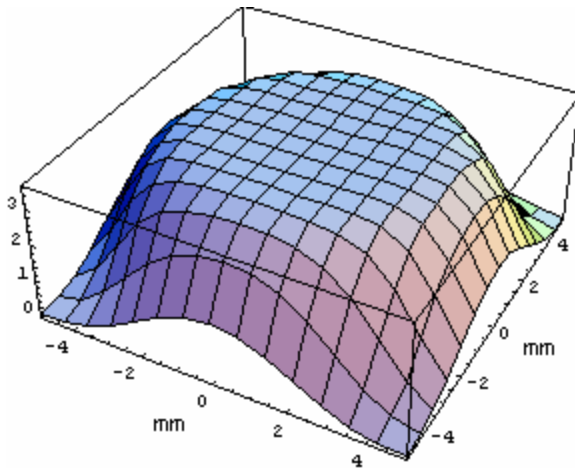


Figure 3.1.3: Sum power falling on QPD of radius = 5mm as a function of the position of the beam centroid across the face of the QPD; Beam waist = 1.5mm

Figures 3.1.4 and 3.1.5 below show how pitch and yaw change as the beam moves across the face of the QPD. Note that when the beam moves very far from the center of the QPD and the total power is reduced, pitch and yaw (as defined by equations 1 and 2) look the same as they do when the beam is perfectly centered. This is why it is always important to note the quadrant sum when determining where on the face of the QPD the beam actually lies.

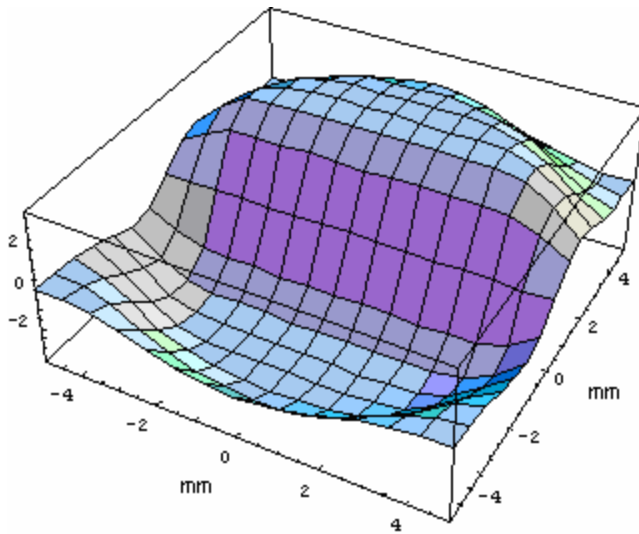


Figure 3.1.4: Pitch

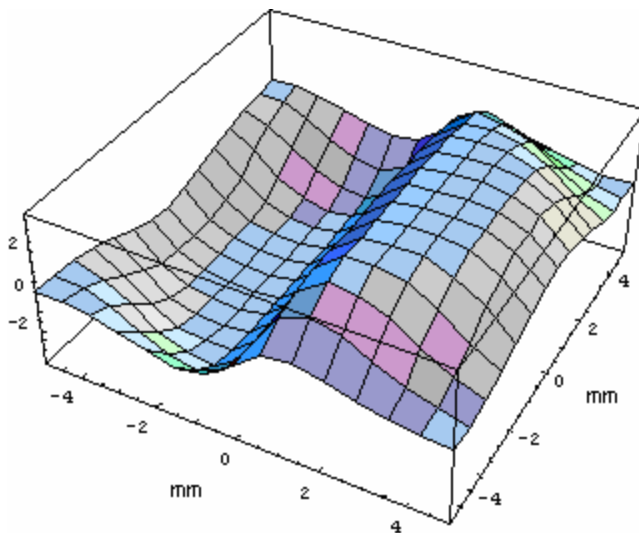


Figure 3.1.5: Yaw

The beams that were being used for the oplevs were in the form of 670nm (red) laser diodes. According to their specifications, the beams were supposed to be Gaussian and circular with a beam waist of 1.5mm. Using a beam scanner to measure the beams of all seven laser diodes, it was found that they were not in fact circular. See Figure 3.1.6.

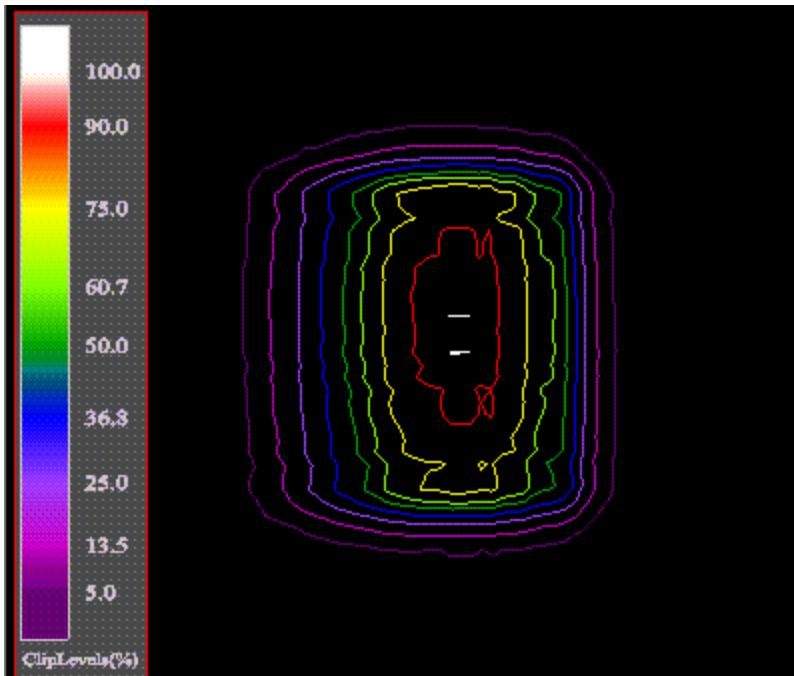


Figure 3.1.6: Beam scan result for all oplev 670nm laser diodes

The rectangular beam shape is most likely the result of the rectangular diode crystal from which the beam is being emitted. In any case, although the quantitative analysis above is no longer accurate, one can still determine the pitch and yaw of the optic, even if the laser is not circular

The movement in QPD face position is proportional to the lever arm and change in angular pitch and/or yaw. Using the equations (equations 3-7) that show how the power (and so voltage), pitch and yaw change with a certain amount of movement across the face of the QPD, it is possible to calibrate the oplevs. As Figures 3.1.4 and 3.1.5 show, pitch and yaw change approximately linearly as the beam moves across the face of the QPD as long as the beam remains close to the center. It can be seen that the range of linear readout of pitch and yaw is approximately $\pm 1.5\text{mm}$ from the center of the QPD. By moving the beam a known amount across the face of a QPD in either pitch or yaw, one can obtain the constants of calibration. In this way, we know exactly how the quadrant voltages change with a certain amount of change in angular pitch and yaw. The determination of these constants for both pitch and yaw was completed only for the BS oplev while I was at the 40m. For the results of this calibration, see Appendix A. Work is now being continued on completing the calibration for the remaining oplevs by my successor, Fumiko Kawazoe.

3.2. Angle-sensing Telescope

An important component of the optical lever system that has been modeled but has yet to be incorporated into the setup is the angle-sensing telescope. This telescope was first mentioned in section 2 of this report, and we will now go into more detail as to its design. The telescope, designed by Michael Smith, combines a variable focal length zoom lens with a collimating lens to form a 6X afocal telescope. The focal length of the zoom lens

varies from 8mm to 48mm. The table below gives the proposed statistics of each lens in succession.

Lens	Radius 1 (mm)	Radius 2 (mm)	Thickness (mm)	Focal Length (mm)
L01				8 - 48
L02	8	-3.1	1.5	6.03218
L1	25.8	8	2	50.2033
L2	8	-1.8		3.50256
L3	25.8	8	2	50.2033
L4	8	-1.8	2	3.50256
L5	12.9	8	4	25.1017

Figure 3.2.1: Table of statistics for lenses in oplev telescope design

(The radius is positive if the beam is approaching a convex surface, negative if approaching a concave surface and 8 if approaching a flat surface.) The QPD is placed at a distance of one focal length from L5. As the focal length of the zoom lens varies from 8mm to 48mm, the Effective Focal Length (EFL) of the telescope varies from 6839.31mm to 41,035.9mm. For the detailed matrix calculations that went into modeling the telescope and determining the EFL, see Appendix B.

4. Assembly of the Optical Lever System

4.1. Mirrors

The actual assembly of each of the optical levers required a significant amount of time and care. Assembly involved cleaning steering mirrors, placing them in their mounts and fixing them to their proper places on the out-of-vacuum oplev tables and the in-vacuum chambers.

The out-of-vacuum oplev mirrors were ordered by Michael Smith from CVI Laser. They were 1"-diameter protected aluminum mirrors suitable for producing high reflectance at 670nm, the wavelength of the oplev laser diodes. The in-vacuum mirrors and mounts were already present at the 40m and did not need to be ordered or assembled. Each of these in-vacuum mirrors were tested to ascertain that they had the appropriate reflectance for a 670nm beam. This beam was reflected off each of the in-vacuum mirrors, and the power of the beam was measured before and after reflectance. Only those mirrors that reflected almost all the total power of the laser diodes were used. All mirrors, both in-vacuum and out, were wiped clean with acetone, then methanol, and finally blown with nitrogen to get rid of any remaining particles.

Figures 4.1.1 and 4.1.2 below show examples of both the in-vacuum and out-of-vacuum setup at the main chamber. The main chamber now houses the BS and BS oplev. In the future the PRM and SRM, as well as their oplevs, will be installed.

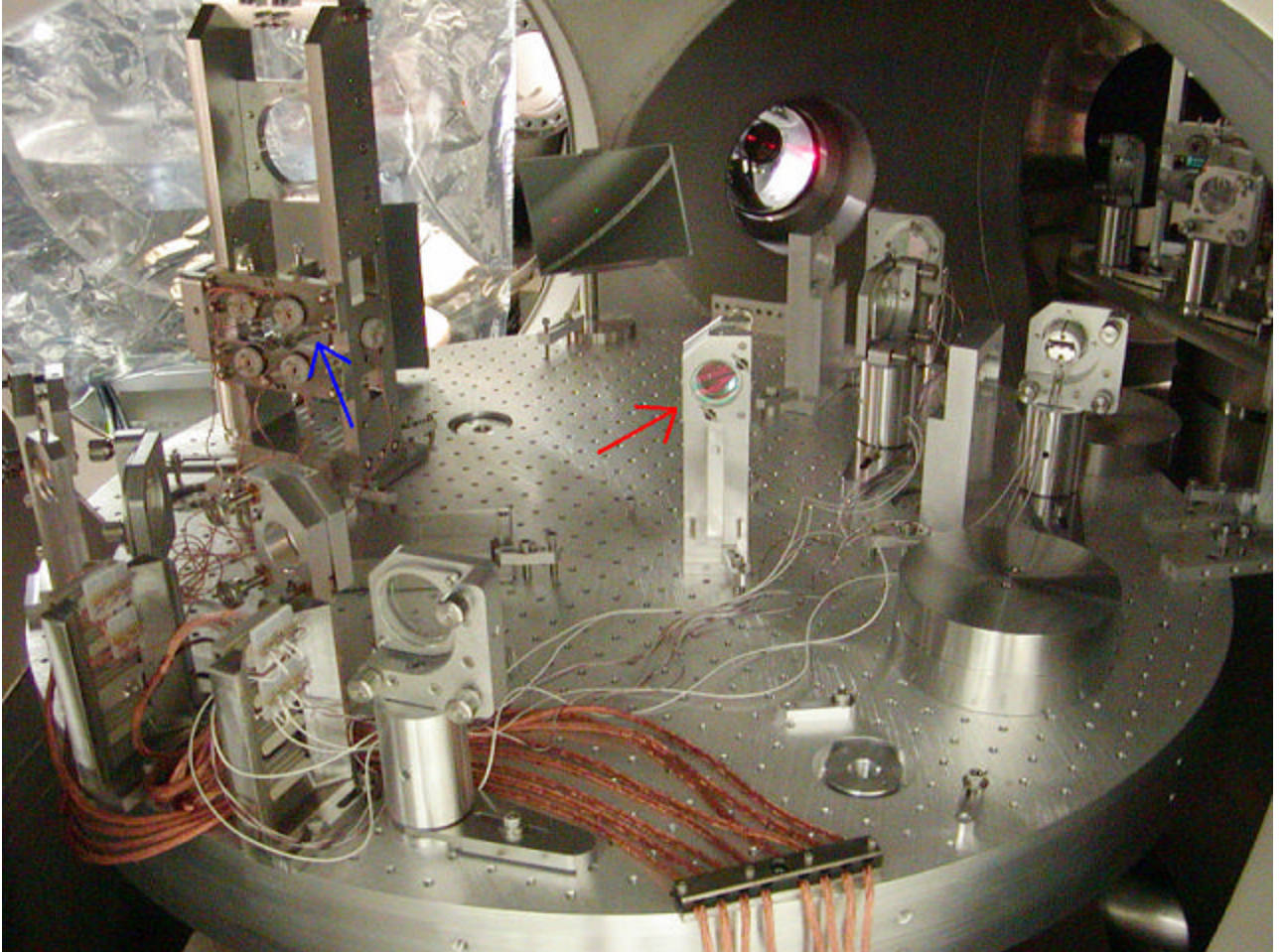


Figure 4.1.1: Main chamber (in-vacuum). The **red** arrow is pointing to one of the in-vacuum oplev steering mirrors. The **blue** arrow is pointing to the BS suspended optic, itself.

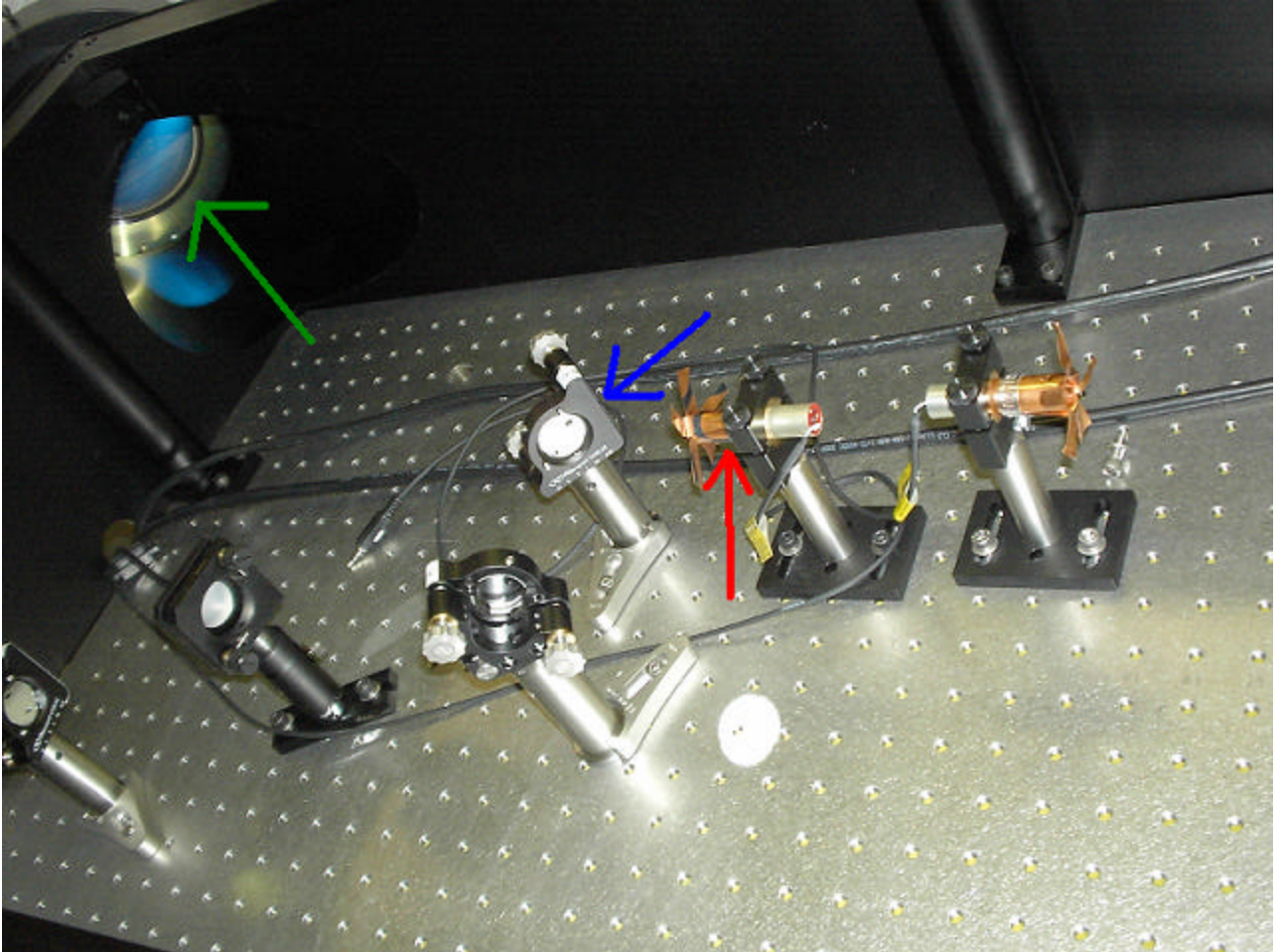


Figure 4.1.2: Oplev table (out-of-vacuum). The **red** arrow is pointing at the laser diode. The **blue** arrow is pointing at one of the out-of-vacuum oplev steering mirrors. The **green** arrow is pointing at the window through the beam enters and exits the main chamber. (The QPD, although present on the table, is not shown here.)

4.2. Beam Path

The actual placement of the laser, mirrors and QPD was not arbitrary. The placement of all the components and the proposed beam path had already been laid out in AutoCAD designs by Michael Smith. Because we were dealing with a Gaussian beam that has a certain beam divergence, meaning the beam radius expands as it travels, it was necessary to use the AutoCAD drawings to calculate estimates of the path lengths. If the path lengths were too long, then the beams hitting the QPDs would be too large. The laser diodes came with a specified beam divergence of 0.40mrad . The diameters of all seven oplev beams as they hit their respective QPDs were calculated using this given beam divergence as well as using the following formula for beam waist as a function of distance traveled, 'z':

$$w(z) = \sqrt{w_0^2 * \left[1 + \left(\frac{\lambda * z}{\pi * w_0^2} \right)^2 \right]}$$

$$\left(\text{divergence} = \theta = \frac{\lambda}{\pi * w_0} \right)$$

Equation 8.1

Equation 8.2

The results of these calculations are shown in Appendix C. Experimental results seemed to concur with the beam radius as calculated using equation 8.1. These radii were in all cases small enough that use of a focusing lens (prior to the installation of the telescope) was unnecessary.

The points on the suspended optics that the oplev beams hit was also far from arbitrary. The ITMs and ETMs are designed to build up resonance in an optical cavity and, therefore, have extremely high reflectances. (BS is designed for 50% reflectance.) These mirrors are also designed to have these high reflectances at 1064nm, the wavelength of the main beam going into the interferometer. Because the oplev beams operate at 670nm, it is important where they hit the suspended optics. (For a more detailed explanation of the wavelength-dependency of the optics, see Appendix D.) The highly reflective dielectric multilayer sections of the suspended optics do not extend to the edge. It is, therefore, desirable for the oplevs to hit the optics close to their edges. When the oplev beams paths were adjusted so they hit the optics in this manner, noticeable increases in power reflected from the optics were observed.

4.3. Electronics

Part of the assembly involved getting the entire electronics chain from the QPD to the EPICS readout up and working. For each oplev, this chain begins with a cable running from the QPD to an oplev interface board. This cable supplies power to the QPD and also receives signals from the four QPD quadrants. Another cable then connects the interface board to a PENTEK ADC (analog-to-digital converter). The ADC is then read out by a Pentium CPU in a VME crate running the VxWorks real-time operating system and is sent via reflective memory to a Linux computer which then sends the signals to an EPICS display. The part of the chain from the PENTEK to EPICS was already set up when I started at the 40m. Getting the electronics chain up and working, therefore, involved getting the cabling all the way from the QPDs to the PENTEKs done, making sure the EPICS displays (see Figure 3.1.2) made sense, and if not, debugging any problems in the code or wiring.

5. Results and Further Work

5.1. Results

Once all oplevs (except those for the yet to be installed PRM and SRM) had been assembled and were in place, the EPICS displays (see figure 3.1.2) clearly showed that they were responding to movement of the suspended optics. The EPICS screen showed that the spots on the QPDs moved accordingly when the optics were driven in pitch or in

yaw. At this point, the calibration constants for the BS oplev have been calculated, and the all oplevs are receiving an accurate signal from the suspended optics and are good measures of how well the optics are being damped.

5.2. Further Work

The final goal in the optical lever project is to “close the loop” by having the oplevs’ signals feedback on the optics to damp their motion. There are small magnets attached to each suspension that push and pull on the suspended optics to damp their motion. This damping, however, occurs at higher frequencies than those at which the oplevs are designed to damp. The oplevs are designed to damp at very low frequencies, less than 10Hz. In order to prevent the oplevs’ damping signals from coming into conflict with the magnets’ damping, it will be necessary to place a frequency filter on the oplev signal. This filter will be such that the oplevs will damp strongly at low frequencies, perhaps below 1Hz. Above this frequency, the oplev damping signal will quickly drop off.

This final phase of the project has yet to be completed. It is assumed that the task of closing the loop for the oplevs will fall to Fumiko Kawazoe.

Acknowledgements

My work this summer would not have been possible without the assistance of my fellow 40m lab mates. I would like to my fellow students, Matthew Eichenfield, Conor Mow-Lowry, Lisa Goggin, and Alexei Ourjountsev for allowing me to benefit from their prior experience in working at LIGO and other optics laboratories. I would also like to thank Steve Vass for helping me with the installation of the in-vacuum optical lever components, Osamu Miyakawa for teaching me how to use much of the equipment in the lab (such as the spectrum analyzer whose result is shown in Figure 3.1.6), Bob Taylor for getting all the cabling done, and Jay Heefner, Ben Abbott and Alex Ivanov for helping me debug the electronics chain. Lastly, I would like to thank my mentor, Alan Weinstein, for giving me this unique and memorable opportunity.

References

Franklin, Powell, Emami-Naeini, Feedback Control of Dynamic Systems, Addison Wesley Publishing Company, 1994.

The LIGO 40m homepage at: http://www.ligo.caltech.edu/~ajw/40m_upgrade.html.

The Melles Griot homepage at: <http://www.mellesgriot.com>.

Siegman, Lasers, University Science Books, 1986.

Smith, Michael, 40 Meter Focal Lengthy Zoom Objective Lens for Optical Lever System-Position Memory, LIGO-T020203-00-D, 6/13/2002.

Zucker, M. E., Calibration of Optical Levers, LIGO-T990026-00-D, 3/5/99.

Appendix A:

For calibration of the BS optical lever, the laser diode beam was sent through a flat glass plate toward the QPD. Starting at 0 degrees, the plate was rotated by known amounts, in intervals of 2 degrees. In this way, the spot on the QPD was shifted. The plate essentially served to represent angular movement of the suspended optic. The data below, in Figures A.1 and A.2, show the data points obtained from the measurements and the results of fitting a straight line to the data: pitch and yaw (as read from the EPICS screen -- see Figure 3.1.2 -- and as defined in equations 1 and 2) versus degrees.

BS oplev pitch calibration

distance from plate to QPD = 13.4 cm

point	x (degrees)	y (pitch)
1	-20.	0.292
2	-16.	0.486
3	-12.	0.611
4	-8.	0.744
5	-4.	0.852
6	0.	0.93

n= 6

LinearFit

n= 6

$$y(x) = a + b x$$

Fit of (x,y) (unweighted)

a= 0.968286 b= 0.0315786

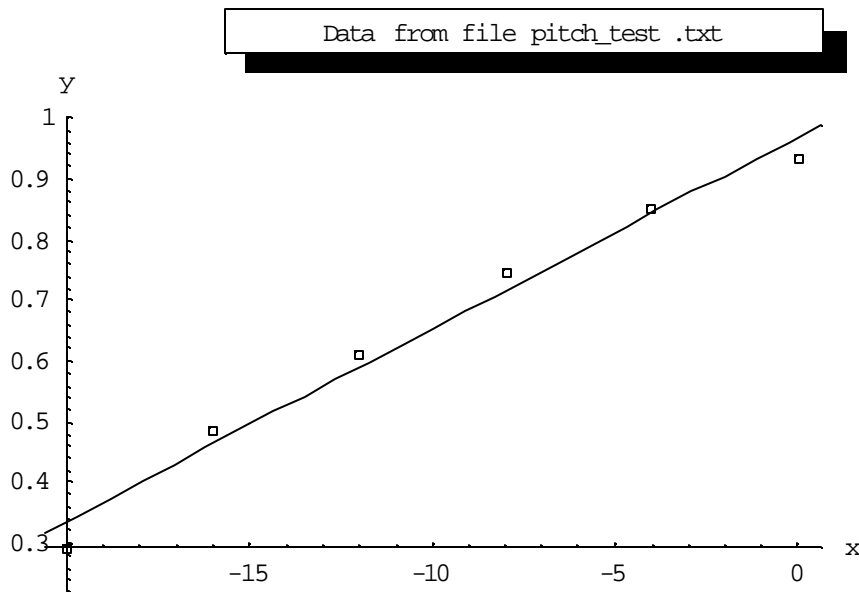


Figure A.1: Linear fit of BS oplev pitch calibration data

BS oplev yaw calibration

distance from plate to QPD = 11.7 cm

point	x (degrees)	y (yaw)
1	0.	-0.386
2	4.	-0.226
3	8.	-0.091
4	12.	0.049
5	16.	0.137

n= 5

LinearFit

n= 5

$$y(x) = a + b x$$

Fit of (x,y) (unweighted)

a= -0.3676 b= 0.033025

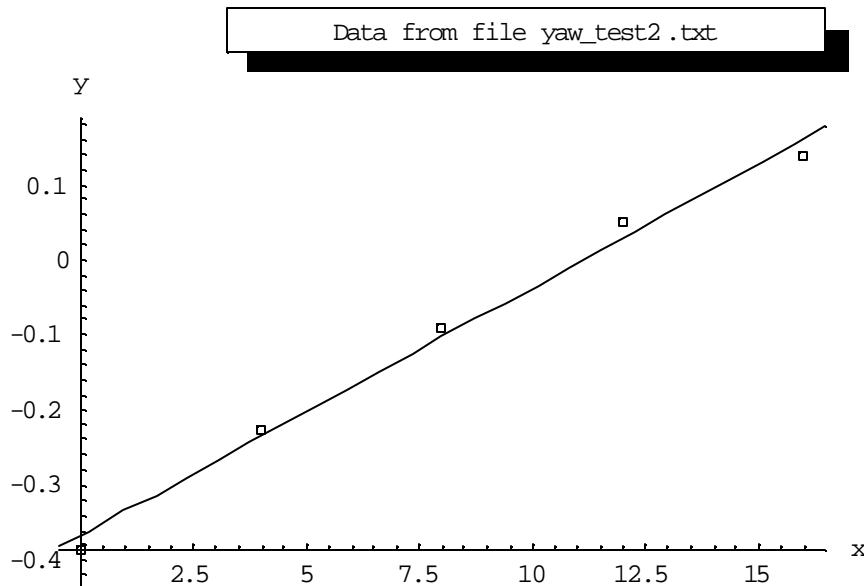


Figure A.2: Linear fit of BS oplev yaw calibration data

These results show that, for the BS oplev,

Pitch = 0.0315786 * degrees and

Yaw = 0.033025 * degrees.

In order to get a dependent variable 'x' that represents displacement on the QPD, we must first take the dependent variable in Figures A.1 and A.2, degrees, and multiply it by (p/180) in order to get the result in units of radians. We must then multiply it by the length of the lever arm (distance from plate to QPD), in order to finally get displacement on the QPD. Figure A.3 below summarizes the results of the calibration.

$$\begin{aligned}
\text{pitch} &= 0.0315786 * \text{degrees} \\
\text{yaw} &= 0.033025 * \text{degrees} \\
\text{displacement on QPD} &= \frac{\pi}{180} * (\text{lever arm}) * \text{degrees} \\
\text{pitch} &= 0.0315786 * \frac{180}{\pi} * \frac{1 \text{ mm}}{134 \text{ mm}} * \text{degrees} \\
\text{pitch} &= 0.013502 * x \\
\text{yaw} &= 0.033025 * \frac{180}{\pi} * \frac{1 \text{ mm}}{117 \text{ mm}} * \text{degrees} \\
\text{yaw} &= 0.016173 * x \\
(x &= \text{displacement on QPD in mm})
\end{aligned}$$

Figure A.3: Results of BS oplev calibration

Appendix B:

OPTICAL LEVER TELESCOPE

(All numerical values below are in units of mm.)

wavelength :

$$\lambda = 0.670 * 10^{(-3)}$$

0.00067

input beam waist size :

$$w0 = 1.5$$

1.5

distance from input beam waist to L01 :

$$s01 = 5000$$

5000

focal length of Lens 01 :

$$FL01 = \{8, 48\}$$

Index of refraction of air :

$$n = 1$$

1

Index of refraction of BK7 lenses :

$$nL = 1.51391$$

1.51391

$$\text{Refract1} := \begin{pmatrix} 1 & 0 \\ (n - nL) / (nL * R1) & n / nL \end{pmatrix}$$

$$\text{Translate} := \begin{pmatrix} 1 & L \\ 0 & 1 \end{pmatrix}$$

$$\text{Refract2} := \begin{pmatrix} 1 & 0 \\ (nL - n) / (n * R2) & nL / n \end{pmatrix}$$

Lens 02 :

$$R1 = \infty$$

∞

$$R2 = -3.1$$

-3.1

$$L = 1.5$$

1.5

Refract1

{{1, 0}, {0, 0.660541}}

Translate

{{1, 1.5}, {0, 1}}

Refract2

{{1, 0}, {-0.165777, 1.51391}}

M02 = Refract2.Translate.Refract1

{{1., 0.990812}, {-0.165777, 0.835746}}

$$a = 1.^{\wedge}$$

1.

$$b = 0.9908118712473^{\wedge}$$

0.990812
c = -0.16577741935483872`
 -0.165777
d = 0.8357457649184838`
 0.835746
location of front principal plane :
r02 = (d-1) / c
 0.990812
location of back principal plane :
s02 = (1-a) / c
 0.
back focal length :
q02 = -a / c
 6.03218
focal length :
FL02 = -1 / c
 6.03218

Lens 1 and Lens 3 :

R1 = 25.8

25.8

R2 = ∞

∞

L = 2

2

Refract1

{{1, 0}, {-0.0131573, 0.660541}}

Translate

{{1, 2}, {0, 1}}

Refract2

{{1, 0}, {0, 1.51391}}

M1 = **Refract2.Translate.Refract1**

{{0.973685, 1.32108}, {-0.019919, 1.}}

M3 = **M1**

{{0.973685, 1.32108}, {-0.019919, 1.}}

a = 0.9736853680231162`

0.973685

b = 1.3210824949964`

1.32108

c = -0.019918992248062022`

-0.019919

d = 1.`

1.

location of front principal plane :

$$r1 = (d - 1) / c$$

0.

location of back principal plane :

$$s1 = (1 - a) / c$$

-1.32108

back focal length :

$$q1 = -a / c$$

48.8823

focal length :

$$FL1 = -1 / c$$

50.2033

Lens 2 and 4 :

$$R1 = \infty$$

∞

$$R2 = -1.8$$

-1.8

$$L = 2$$

2

Refract1

$$\{\{1, 0\}, \{0, 0.660541\}\}$$

Translate

$$\{\{1, 2\}, \{0, 1\}\}$$

Refract2

$$\{\{1, 0\}, \{-0.285506, 1.51391\}\}$$

M2 = Refract2.Translate.Refract1

$$\{\{1., 1.32108\}, \{-0.285506, 0.622824\}\}$$

M4 = M2

$$\{\{1., 1.32108\}, \{-0.285506, 0.622824\}\}$$

a = 1.

1.

b = 1.3210824949964

1.32108

c = -0.2855055555555556

-0.285506

d = 0.6228236083313333

0.622824

location of front principal plane :

$$r2 = (d - 1) / c$$

1.32108

location of back principal plane :

$$s2 = (1 - a) / c$$

0.

back focal length :

$$q2 = -a / c$$

3.50256

focal length :

$$FL2 = -1 / c$$

3.50256

Lens 5 :

$$R1 = 12.9$$

12.9

$$R2 = \infty$$

∞

$$L = 4$$

4

Refract1

{{1, 0}, {-0.0263146, 0.660541}}

Translate

{{1, 4}, {0, 1}}

Refract2

{{1, 0}, {0, 1.51391}}

M5 = Refract2.Translate.Refract1

{{0.894741, 2.64216}, {-0.039838, 1.}}

$$a = 0.8947414720924651^{\sim}$$

0.894741

$$b = 2.6421649899928^{\sim}$$

2.64216

$$c = -0.039837984496124045^{\sim}$$

-0.039838

$$d = 1.^{\sim}$$

1.

location of front principal plane :

$$r5 = (d - 1) / c$$

0.

location of back principal plane :

$$s5 = (1 - a) / c$$

-2.64216

back focal length :

$$q5 = -a / c$$

22.4595

focal length :

$$FL5 = -1 / c$$

25.1017

defocus between L01 and L02 :

$\Delta 0102$

distance between L01 and L02 :

$$l_{0102} = FL01 + FL02 - r02 + \Delta 0102$$

$$5.04137 + FL01 + \Delta 0102$$

distance between L02 and L1 :

$$l_{021} = 1$$

1

distance between L1 and L2 :

$$l_{12} = FL1 + FL2 + s1 - r2$$

$$51.0637$$

l_{12}

$$51.0637$$

distance between L2 and L3 :

$$l_{23} = l_{021}$$

1

l_{23}

1

distance between L3 and L4 :

$$l_{34} = l_{12}$$

$$51.0637$$

l_{34}

$$51.0637$$

distance between L4 and L5 :

$$l_{45} = FL5$$

$$25.1017$$

l_{45}

$$25.1017$$

distance between L5 and QPD :

$$l_{QPD} = FL5 + s5$$

$$22.4595$$

l_{QPD}

$$22.4595$$

Translate from laser diode input to L01 :

$$T01 = \begin{pmatrix} 1 & s01 \\ 0 & 1 \end{pmatrix}$$

$$\{\{1, 5000\}, \{0, 1\}\}$$

T01

$$\{\{1, 5000\}, \{0, 1\}\}$$

Lens L01 (thin lens) matrix :

$$M01 = \begin{pmatrix} 1 & 0 \\ -1/FL01 & 1 \end{pmatrix}$$

$$\left\{ \{1, 0\}, \left\{ -\frac{1}{\text{FL01}}, 1 \right\} \right\}$$

M01[FL01]

$$\left\{ \{1, 0\}, \left\{ -\frac{1}{\text{FL01}}, 1 \right\} \right\} [\text{FL01}]$$

Translate from L01 to L02 :

$$\mathbf{T02} = \begin{pmatrix} 1 & l_{0102} \\ 0 & 1 \end{pmatrix}$$

$$\{ \{1, 5.04137 + \text{FL01} + \Delta 0102\}, \{0, 1\} \}$$

Lens L02 matrix :

M02

$$\{ \{1., 0.990812\}, \{-0.165777, 0.835746\} \}$$

Translate from L02 to L1 :

$$\mathbf{T1} = \begin{pmatrix} 1 & l_{021} \\ 0 & 1 \end{pmatrix}$$

$$\{ \{1, 1\}, \{0, 1\} \}$$

T1

$$\{ \{1, 1\}, \{0, 1\} \}$$

Lens L1 matrix :

M1

$$\{ \{0.973685, 1.32108\}, \{-0.019919, 1.\} \}$$

Translate from L1 to L2 :

$$\mathbf{T2} = \begin{pmatrix} 1 & l_{12} \\ 0 & 1 \end{pmatrix}$$

$$\{ \{1, 51.0637\}, \{0, 1\} \}$$

T2

$$\{ \{1, 51.0637\}, \{0, 1\} \}$$

Lens L2 matrix :

M2

$$\{ \{1., 1.32108\}, \{-0.285506, 0.622824\} \}$$

Translate from L2 to L3 :

$$\mathbf{T3} = \begin{pmatrix} 1 & l_{23} \\ 0 & 1 \end{pmatrix}$$

$$\{ \{1, 1\}, \{0, 1\} \}$$

T3

$$\{ \{1, 1\}, \{0, 1\} \}$$

Lens L3 matrix :

M3

$$\{ \{0.973685, 1.32108\}, \{-0.019919, 1.\} \}$$

Translate from L3 to L4 :

$$\mathbf{T4} = \begin{pmatrix} 1 & l_{34} \\ 0 & 1 \end{pmatrix}$$

$$\{ \{1, 51.0637\}, \{0, 1\} \}$$

T4

$$\{ \{1, 51.0637\}, \{0, 1\} \}$$

Lens L4 matrix :

M4

{{1., 1.32108}, {-0.285506, 0.622824}}

Translate from L4 to L5 :

$$T5 = \begin{pmatrix} 1 & L_{45} \\ 0 & 1 \end{pmatrix}$$

{{1, 25.1017}, {0, 1}}

T5

{{1, 25.1017}, {0, 1}}

Lens L5 matrix :

M5

{{0.894741, 2.64216}, {-0.039838, 1.}}

Translate from L5 to QPD :

$$T_{QPD} = \begin{pmatrix} 1 & L_{QPD} \\ 0 & 1 \end{pmatrix}$$

{{1, 22.4595}, {0, 1}}

T_{QPD}

{{1, 22.4595}, {0, 1}}

System matrix at QPD :

M_{QPD} = T_{QPD}.M5.T5.M4.T4.M3.T3.M2.T2.M1.T1.M02.T02.M01.T01

$$\left\{ \left\{ -854.914 - \frac{4309.94 - 854.914 (5.04137 + FL01 + \Delta 0102)}{FL01}, \right. \right. \\ \left. \left. 4309.94 - 854.914 (5.04137 + FL01 + \Delta 0102) + \right. \right. \\ \left. \left. 5000 \left(-854.914 - \frac{4309.94 - 854.914 (5.04137 + FL01 + \Delta 0102)}{FL01} \right) \right\}, \right. \\ \left\{ -5.10214 - \frac{25.7206 - 5.10214 (5.04137 + FL01 + \Delta 0102)}{FL01}, \right. \\ \left. 25.7206 - 5.10214 (5.04137 + FL01 + \Delta 0102) + \right. \\ \left. 5000 \left(-5.10214 - \frac{25.7206 - 5.10214 (5.04137 + FL01 + \Delta 0102)}{FL01} \right) \right\} \left. \right\}$$

$$\begin{pmatrix} MS_{00} & MS_{01} \\ MS_{10} & MS_{11} \end{pmatrix} = M_{QPD}$$

$$\left\{ \left\{ -854.914 - \frac{4309.94 - 854.914 (5.04137 + FL01 + \Delta 0102)}{FL01}, \right. \right. \\ \left. \left. 4309.94 - 854.914 (5.04137 + FL01 + \Delta 0102) + \right. \right. \\ \left. \left. 5000 \left(-854.914 - \frac{4309.94 - 854.914 (5.04137 + FL01 + \Delta 0102)}{FL01} \right) \right\}, \right. \\ \left\{ -5.10214 - \frac{25.7206 - 5.10214 (5.04137 + FL01 + \Delta 0102)}{FL01}, \right. \\ \left. 25.7206 - 5.10214 (5.04137 + FL01 + \Delta 0102) + \right. \\ \left. 5000 \left(-5.10214 - \frac{25.7206 - 5.10214 (5.04137 + FL01 + \Delta 0102)}{FL01} \right) \right\} \left. \right\}$$

MS₀₀

$$-854.914 - \frac{4309.94 - 854.914 (5.04137 + FL01 + \Delta 0102)}{FL01}$$

MS₀₁

$$4309.94 - 854.914 (5.04137 + FL01 + \Delta 0102) +$$

$$5000 \left(-854.914 - \frac{4309.94 - 854.914 (5.04137 + FL01 + \Delta 0102)}{FL01} \right)$$

MS₁₀

$$-5.10214 - \frac{25.7206 - 5.10214 (5.04137 + FL01 + \Delta 0102)}{FL01}$$

MS₁₁

$$25.7206 - 5.10214 (5.04137 + FL01 + \Delta 0102) +$$

$$5000 \left(-5.10214 - \frac{25.7206 - 5.10214 (5.04137 + FL01 + \Delta 0102)}{FL01} \right)$$

input ray height at 0 :

$$h_0 = 0$$

0

input ray angle at L1 (rad) :

$$\alpha_0 = 0.2 \times 10^{-6}$$

$$2. \times 10^{-7}$$

$$h_{QPD} = MS_{00} * h_0 + MS_{01} * \alpha_0$$

$$2. \times 10^{-7} \left(4309.94 - 854.914 (5.04137 + FL01 + \Delta 0102) + \right.$$

$$\left. 5000 \left(-854.914 - \frac{4309.94 - 854.914 (5.04137 + FL01 + \Delta 0102)}{FL01} \right) \right)$$

$$\alpha_{QPD} = MS_{10} * h_0 + MS_{11} * \alpha_0$$

$$2. \times 10^{-7} \left(25.7206 - 5.10214 (5.04137 + FL01 + \Delta 0102) + \right.$$

$$\left. 5000 \left(-5.10214 - \frac{25.7206 - 5.10214 (5.04137 + FL01 + \Delta 0102)}{FL01} \right) \right)$$

Effective Focal Length :

$$EFL = h_{QPD} / \alpha_0$$

$$1. \left(4309.94 - 854.914 (5.04137 + FL01 + \Delta 0102) + \right.$$

$$\left. 5000 \left(-854.914 - \frac{4309.94 - 854.914 (5.04137 + FL01 + \Delta 0102)}{FL01} \right) \right)$$

QPD beam waist

system matrix to QPD beam waist :

$$w_{QPD} =$$

$$\left((\lambda / \pi) * ((-MS_{01}^2) - MS_{00}^2 * (\pi * w_0^2 / \lambda)^2) / ((\pi * w_0^2 / \lambda) * (MS_{01} * MS_{10} - MS_{00} * MS_{11})) \right)$$

$$0.5$$

$$\begin{aligned}
& 0.000142178 \left(\left(-1.11305 \times 10^8 \left(-854.914 - \frac{4309.94 - 854.914 (5.04137 + FL01 + \Delta 0102)}{FL01} \right) \right)^2 - \right. \\
& \quad \left(4309.94 - 854.914 (5.04137 + FL01 + \Delta 0102) + \right. \\
& \quad \quad \left. 5000 \left(-854.914 - \frac{4309.94 - 854.914 (5.04137 + FL01 + \Delta 0102)}{FL01} \right) \right)^2 \Bigg) / \\
& \left(\left(-5.10214 - \frac{25.7206 - 5.10214 (5.04137 + FL01 + \Delta 0102)}{FL01} \right) \right. \\
& \quad \left(4309.94 - 854.914 (5.04137 + FL01 + \Delta 0102) + \right. \\
& \quad \quad \left. 5000 \left(-854.914 - \frac{4309.94 - 854.914 (5.04137 + FL01 + \Delta 0102)}{FL01} \right) \right) - \\
& \quad \left(-854.914 - \frac{4309.94 - 854.914 (5.04137 + FL01 + \Delta 0102)}{FL01} \right) \\
& \quad \left(25.7206 - 5.10214 (5.04137 + FL01 + \Delta 0102) + \right. \\
& \quad \quad \left. 5000 \left(-5.10214 - \frac{25.7206 - 5.10214 (5.04137 + FL01 + \Delta 0102)}{FL01} \right) \right) \Bigg) \Bigg)^{0.5}
\end{aligned}$$

Length of objective lens :

$$L_L = l_{0102} + l_{021} + l_{12} + l_{23} + l_{34} + l_{45} + l_{OPD} + 1.5 + 2 + 2 + 2 + 2 + 4$$

$$170.23 + FL01 + \Delta 0102$$

$$\Delta 0102 = 0$$

$$0$$

$$FL01 = 8$$

$$8$$

EFL

$$-6839.31$$

$$FL01 = 48$$

$$48$$

EFL

$$-41035.9$$

Appendix C:

Beam diameter = 3.0 mm = $2 \cdot W_0$
 Beam divergence = 0.40 mrad using Steve's 670nm laser diodes
 QPD diameter = 10 mm

	BS	PRM	SM	ITM _x	ITM _y	ETM _x	ETM _y	
	Total path lengths (mm)							
<i>z</i>	5794.314	5095.552	5599.933	3662.911	4058.275	5033.988	5024.206	(without telescope)
	Waists calculated using beam divergence = 0.40mrad:							
<i>w(z)</i>	2.76077	2.53068	2.69583	2.09683	2.21023	2.51089	2.50775	
$2 \cdot w(z)$	5.52154	5.06136	5.39166	4.19366	4.42046	5.02178	5.0155	
	Waists calculated using beam divergence as defined in equation 8.2:							
<i>w(z)</i>	1.71134	1.66579	1.69821	1.58783	1.60715	1.66201	1.66141	
$2 \cdot w(z)$	3.42268	3.33158	3.39642	3.17566	3.2143	3.32402	3.32282	

As is seen in the last row of the above table, the diameters of the beams for each oplev when they reach the QPDs are all only slightly greater than the initial beam waists of 3.0mm. As the diameter of each QPD is 10mm, a maximum beam diameter of 3.42268mm for the BS oplev is small enough to fit entirely within the range of the photodetector, leaving ample room for movement if the angular orientation of the suspended optic is disturbed.

Appendix D:

LIGO's suspended optics are made highly reflective for a specific wavelength using a method of dielectric stacking. Quarter wavelength thicknesses of alternately high and low refractive index materials are stacked upon each other and applied to a substrate. Since each layer is chosen to be a quarter wavelength thick for some particular wavelength, alternate reflections are phase shifted by 180° because they occur at low-to-high-index interfaces. These phase shifts are exactly canceled by the 180° phase shifts caused by the path difference between alternate reflecting surfaces. By choosing materials of appropriate refractive indices, the various reflected wave fronts are then exactly in phase and can be made to interfere constructively in order to produce a highly efficient reflector. The reflectance can be increased by adding more layers of dielectric.

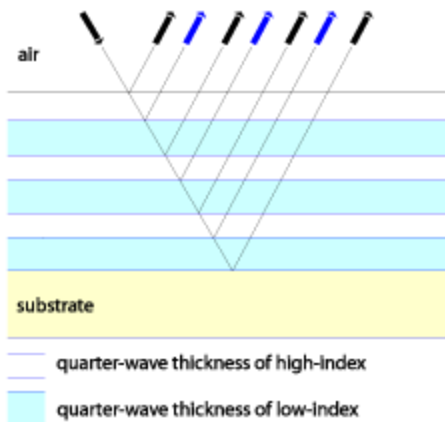


Figure C.1: Quarter-wave dielectric stack

The amplitude reflectivity at a single interface is given by Equations C.1 and C.2:

$$\frac{(1 - p)}{(1 + p)} \quad \text{Equation C.1}$$

$$p = \left(\frac{n_H}{n_L} \right)^{N-1} * \frac{n_H^2}{n_S} \quad \text{Equation C.2}$$

n_H = index of high - index layer

n_L = index of low - index layer

n_S = index of substrate

N = total number of layers in stack

The quarter-wave stacks in the optics at the 40m are designed for 1064nm. This is why they have very low reflectances at the oplev wavelength of 670nm.